10-18-2022

Insight into nano-chemical enhanced oil recovery from carbonate reservoirs using environmentally friendly nanomaterials

Ali Ahmadi

Abbas Khaksar Manshad

Jagar A. Ali

Stefan Iglauer
Edith Cowan University, s.iglauer@ecu.edu.au

S. Mohammad Sajadi

See next page for additional authors

10.1021/acsomega.2c03076
Ahmadi, A., Manshad, A. K., Ali, J. A., Iglauer, S., Sajadi, S. M., Keshavarz, A., & Mohammadi, A. H. (2022). Insight into nano-chemical enhanced oil recovery from carbonate reservoirs using environmentally friendly nanomaterials. *ACS omega*, 7(41), 36165-36174.
https://doi.org/10.1021/acsomega.2c03076

ACS OMEGA

http://pubs.acs.org/journal/acsodf

Article

Insight into Nano-chemical Enhanced Oil Recovery from Carbonate Reservoirs Using Environmentally Friendly Nanomaterials

Ali Ahmadi, Abbas Khaksar Manshad,* Jagar A. Ali, Stefan Iglauer, S. Mohammad Sajadi, Alireza Keshavarz, and Amir H. Mohammadi*

Cite This: *ACS Omega* 2022, 7, 36165−36174

Read Online

ACCESS | Metrics & More | Article Recommendations

ABSTRACT: The use of nanoparticles (NPs) in enhanced oil recovery (EOR) processes is very effective in reducing the interfacial tension (IFT) and surface tension (ST) and altering the wettability of reservoir rocks. The main purpose of this study was to use the newly synthesized nanocomposites (KCl/SiO_2/Xanthan NCs) in EOR applications. Several analytical techniques including X-ray diffraction (XRD), Fourier transform infrared spectroscopy (FTIR), and scanning electron microscope (SEM) were applied to confirm the validity of the synthesized NCs. From the synthesized NCs, nanofluids were prepared at different concentrations of 100−2000 ppm and characterized using electrical conductivity, IFT, and ST measurements. From the obtained results, it can be observed that 1000 ppm is the optimal concentration of the synthesized NCs that had the best performance in EOR applications. The nanofluid with 1000 ppm KCl/SiO_2/Xanthan NCs enabled reducing the IFT and ST from 33 and 70 to 29 and 40 mN/m, respectively. However, the contact angle was highly decreased under the influence of the same nanofluid to 41° and the oil recovery improved by an extra 17.05% OOIP. To sum up, KCl/SiO_2/Xanthan NCs proved highly effective in altering the wettability of rocks from oil-wet to water-wet and increasing the cumulative oil production.

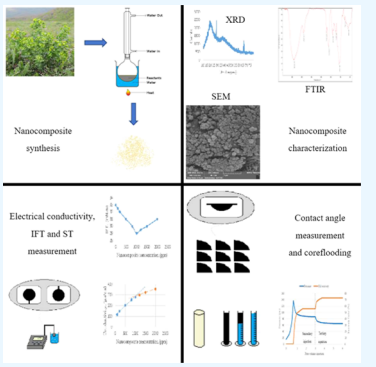

1. INTRODUCTION

Oil and gas companies have been attempting to improve oil recovery from mature reservoirs due to the increase in demand for fossil fuels and the reduction of unexplored hydrocarbon reservoirs in the world.[1,2] The exploration and exploitation of new reservoirs are riskier and costly compared with using enhanced oil recovery (EOR) methods.[3,4] There are primary, secondary, and tertiary methods for producing oil from oil reservoirs. During first two phases of oil extraction, only about 30−50% original oil in place (OOIP) of the crude oil can be produced depending on the characteristics of the reservoir.[5,6] Since only about 30−50% OOIP can be extracted from the reservoirs using the primary and secondary methods, tertiary (EOR) methods are given more attention.[7−9] There are several techniques for producing oil using the tertiary method, such as chemical injection, gas injection, thermal methods, and microbial methods.[10] The chemical EOR (CEOR) processes can be activated by the dominant mechanisms of EOR, such as mobility control, wettability alteration, and interfacial tension (IFT) reduction.[11−13]

The high capillary force in the reservoirs causes small droplets of oil to be trapped in the pore structure. The capillary force prevents oil from moving through the small pore throats.[14] Therefore, reducing and limiting this force will cause trapped oil to become free in the porous media and significantly increase oil recovery. Reduction of capillary force in the reservoir is highly dependent on the values of the IFT between water and oil and the contact angle of crude oil in the presence of the water phase. Two neighboring immiscible fluids form a curved surface due to the tension between their surfaces, and the pressure difference along the curved surface of these two fluids in a capillary tube is the capillary pressure. In recent years, with the development and expansion of nanoscience, researchers in all fields have been attracted to this technology in food and textiles industries, biomedicine, electronics, chemistry, materials, and so on. In the oil industry, especially reservoir engineering, nanotechnology has gained special importance and has been tested with different EOR methods.[15,16] Norio introduced the term nanotechnology to provide ultrafine sizes (1−100 nm) with high accuracy. He described nanotechnology as the process of separating, consolidating, and deforming materials by one atom or one molecule.[9,17,18] Solid phases with at least one nanometer-sized dimension in a three-dimensional space are known as nanoparticles. Nanomaterials are attractive due to their superior properties, such as better dispersion rate and range of activity

Received: May 17, 2022
Accepted: August 19, 2022
Published: October 9, 2022

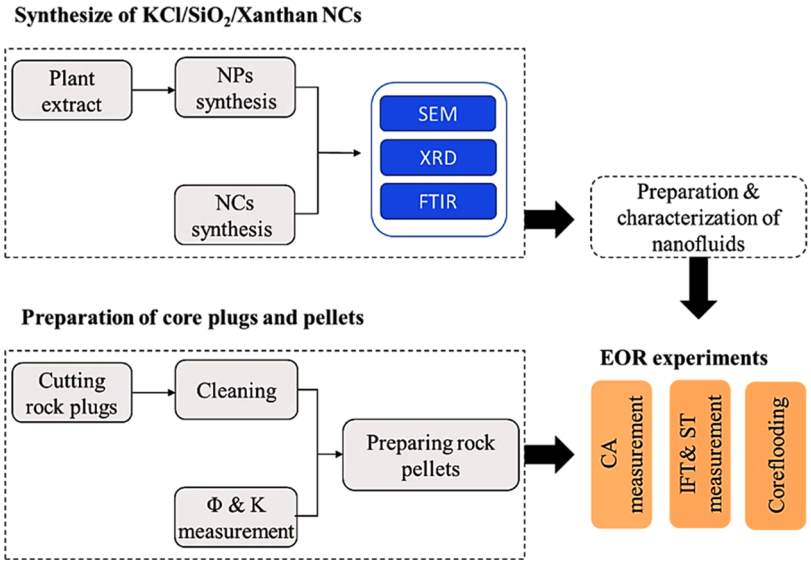

Figure 1. Schematic illustration of the design of experiment (procedural steps of the experimental work) used in this study.

and contact with adjacent surfaces due to having a large surface area.[9]

In EOR, the use of nanomaterials and research on the promotion of various EOR methods by these materials has increased rapidly, especially since 2009.[19] Nano-enhanced oil recovery (NEOR) is usually combined with other methods such as chemical methods, smart water at low and high salinity, carbonated water injection (CWI), gas injection, foam flooding, and polymer or alkaline surfactant polymer (ASP) injection. As per research and field experiences, these processes have shown several problems, such as instability, degradation, high concentration, cost, and adsorption. Thus, oil companies as well as researchers use nanotechnology to overcome these problems.[20,21] The use of nanoparticles (NPs) in various EOR processes can increase oil recovery with positive influences on chemical adsorption, IFT reduction, and wettability alteration. In addition, NPs can easily transfer through the small pore exit in porous media, increase the viscosity and conductivity of solutions, improve the properties of the carrier fluid with a small amount of material compared to materials with larger particles, and make no changes in the chemistry of injected water.[22−26] Furthermore, nanocomposites, as a combination of several NPs or NPs with polymers having the inherent properties of composite materials in intensified states, are expected to perform better in EOR applications compared with conventional nanoparticles (SiO_2, TiO_2, ZnO, Al_2O_3, Fe_2O_3, and graphene).[7−31] Nanocomposites can be functionalized, polymer-coated, or surface-modified nanoparticles.[32,33] Ju et al.[35] and Qi et al.[36] used polymer-coated silica NPs to increase oil recovery by reducing the IFT and altering the wettability.[35,36] Behzadi et al.[37] investigated the effect of polymer-coated silica NPs on the reduction of the water−oil IFT and wettability alteration using a glass micromodel. They identified that polymer-coated silica NPs have a greater impact on the EOR mechanisms compared with unmodified silica NPs.[37]

In other research studies, the effects of other reservoir parameters including temperature and salinity were considered.[38−41] Bila et al.[34] found that temperature and salinity have a low influence on the performance of the nanomaterials when they applied polymer-coated silica NPs.[33] In addition, the effects of the size of silica NPs and silica−xanthan NCs were studied by Ragab et al.[19] They concluded that the smaller NPs have a higher impact on increasing the oil recovery compared with NPs with a larger size.[19] Jafarbeigi et al.[42] studied the impact of the modified graphene oxide (GO) nanofluid on wettability and IFT during EOR. They reported that the used nanofluid can change both the IFT and wettability due to improving the sweep efficiency.[42] The effect of silica NPs combined with xanthan gum on the wettability of carbonate rocks with different water saturations was studied by Soliman et al.[43] In our previous publications on the synthesis and application of nanocomposites in EOR applications, the effects of salinity, pressure, and temperature were investigated.[44−46] From the outcomes of these studies, it was concluded that temperature has a direct influence on the performance of nanomaterials in reducing the IFT and altering the wettability toward water-wet. However, pressure and salinity had an inverse impact on the NP performance for EOR applications.[44−47] The ultimate goal of this study was to synthesize KCl/SiO_2/Xanthan NCs in a green way for EOR applications. The validity of the synthesized NCs was confirmed using scanning electron microscope (SEM), X-ray diffraction (XRD), and Fourier transform infrared spectroscopy (FTIR) analytical techniques. From the confirmed NCs, nanofluid solutions were developed for IFT reduction and wettability alteration. In addition, the most effective nanofluid with the optimal concentration of KCl/SiO_2/xanthan NCs was applied for the enhancement of oil recovery using the oil displacement method.

2. MATERIALS AND METHODS

The procedural steps of the experimental work are shown in Figure 1. In this study, nanocomposites were synthesized and characterized, as mentioned earlier. In addition, rock plugs and pellets were prepared, cleaned, and characterized. Afterward, the EOR experiments including the IFT, surface tension (ST), CA, and oil recovery measurements were performed.

2.1. Fluid and Rock Samples. A cylinder containing pure CO_2 gas was used for surface tension (ST) measurements in this study. A light crude oil with the density of 0.84 g/cm^3 and 36.95° API was collected from the Ahvaz oilfield in the southwest of Iran. The composition and main features of the crude oil are given in Table 1. As can be seen, methane is the dominant

https://doi.org/10.1021/acsomega.2c03076
ACS Omega 2022, 7, 36165−36174

Table 1. Composition and Main Characteristics of the Crude Oil[abcde]

component	C_1	C_2	C_3	iC_4	nC_4	iC_5	nC_5	C_6	C_7	C_8	C_9	C_{10}	C_{11}	C_{12^+}
molar percent	45.73	7.91	5.34	1.12	2.93	1.02	1.14	3.83	3.34	2.48	3.03	2.19	1.78	18

[a]API° = 36.95°. [b]Molecular weight of C_{12^+} = 330 (g/mol). [c]Density of C_{12^+} = 0.9214 (g/mL). [d]Molecular weight of reservoir oil = 94 (g/mol). [e]Gas-to-oil ratio (GOR) = 914.14 ft^3/bbl.

Table 2. Composition of the Seawater and Formation Water Used in the Study

	concentration [ppm]							
component	Na^+	K^+	Mg^{2+}	Ca^{2+}	Fe^{2+}	Cl^-	HCO_3	SO_4
seawater[a]	64	2.37	78	96	0.42	324	166	143.6
formation water[b]	57,031	57,031	1701	9000	0	108,275	220	768

[a]Total hardness = 8700 ppm; TDS = 33.194 mg/L. [b]TDS (mg/lit) = 176,995; viscosity (cp) = 1.22 cP.

Table 3. Characteristics of the Core Plug Prepared from the Collected Rock Samples

diameter (cm)	length (cm)	bulk volume (cm^3)	dry weight (g)	water-wet weight (g)	pore volume (cm^3)	porosity (%)	permeability (mD)
3.72	7.5	81.47	191.47	201.57	9.31	11.43	7.3

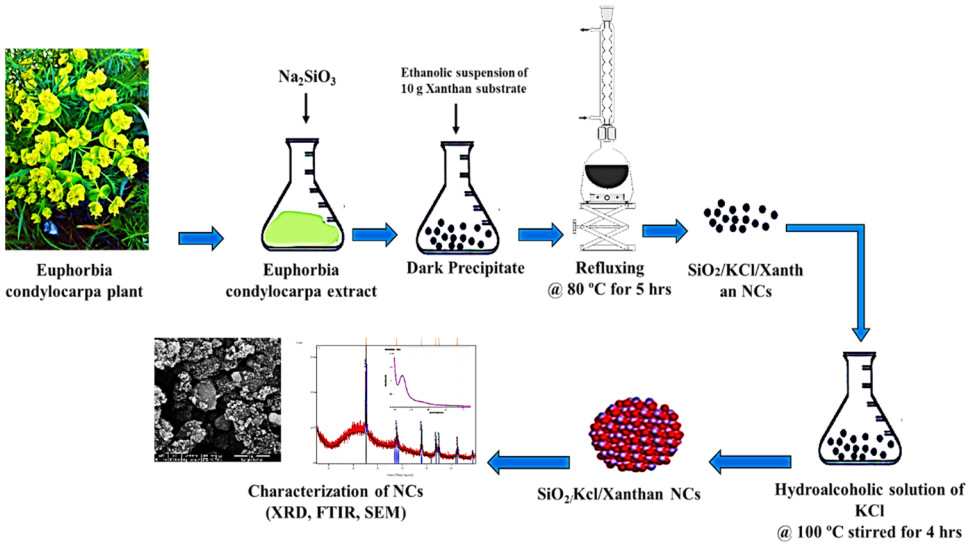

Figure 2. Schematic illustration of the procedural steps of the synthesis of NCs. Reprinted with permission from [Ali, et al., 2022].[47] Copyright [2022/ Energy & Fuels] [American Chemical Society].

compound, accounting for 45.73%. In addition, distilled water with an electrical conductivity of 3.4 μs/cm and a pH of 5.82 and seawater collected from the Persian Gulf, with the composition listed in Table 2, were used in this study. The formation water, with the properties given in Table 2, was collected from the Asmari reservoir that was used to saturate the core that its.

2.2. Rock Sample. Several rock samples were collected from the Asmari Outcrop in southwest Iran. The collected rock samples were taken from the carbonate formation. Core plugs and pellets were prepared from the used rock samples for conducting the contact angle and displacement tests. The physical properties of the core plug prepared for oil displacement are given in Table 3. As can be seen, the porosity of the used core plug is 11.43% and the permeability is 7.3 mD. The porosity and permeability were measured using a standard porosity meter and a permeameter, respectively.

2.3. Synthesis of KCl/SiO_2/Xanthan Nanocomposites. Figure 2 illustrates the procedural steps of synthesizing SiO_2/KCl/Xanthan NCs in a green way.[46−48] In this method, 100 g of dried leaves of the *Euphorbia condylocarpa* plant was mixed with 500 mL of distilled water for 30 min at 80 °C to produce the extract. To develop the silica NPs, 5 g of Na_2SiO_3 was mixed with 100 mL of the collected extract for 10 h under the experimental condition of 10 pH and 80 °C. The stirring was continued until a dried precipitate was obtained and then mixed with 100 mL of a KCl-hydroalcoholic solution under the same experimental condition.[12] Afterward, the obtained powder mixture of silica NPs and KCl was mixed with 10 g of xanthan as a substrate using a refluxing system for 5 h in the presence of ethanol. The collected nanopowder from the reflux was then dried and analyzed by XRD, FTIR, and SEM.

2.4. Preparation of Nanofluids. Nanofluids are those fluids that contain nanomaterials as dispersion particles, which are mixed using a hot plate stirrer and/or a homogenizer.[32] A two-step method was used to prepare stable nanofluids by dispersing SiO_2/KCl/Xanthan NCs with water at different concentrations of 100, 200, 500, 800, 1000, 1200, 1500, and 2000 ppm. In this way, a certain amount of nanocomposite powder was first weighed by a digital laboratory scale and mixed with distilled water and stirred on an MS7-H550-S Model magnetic stirrer. In the next step, ultrasonic agitation was used to disperse nanomaterials in distilled water and prepare stable nanofluids.[33] After adding the synthesized NCs to distilled water to prevent primary agglomeration or cluster of nanoparticles, the

https://doi.org/10.1021/acsomega.2c03076
ACS Omega 2022, 7, 36165−36174

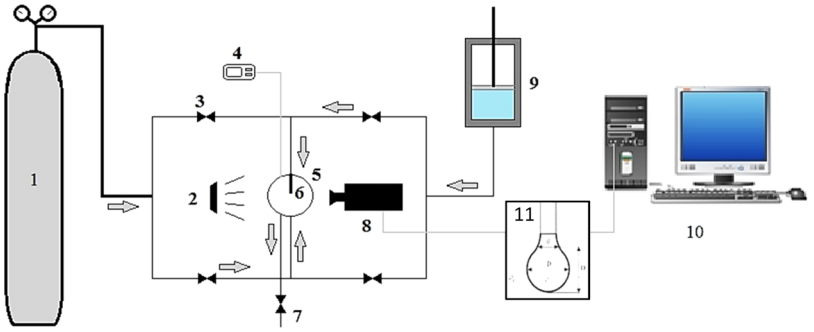

Figure 3. Schematic illustration of the setup of the VIT 6000 device. (1) CO_2 gas cylinder, (2) light source, (3) valve, (4) indicator and temperature and pressure controller, (5) cell, (6) drop needle, (7) cell content drainage line, (8) camera, (9) drop fluid pump, (10) computer, and (11) crude oil droplet.

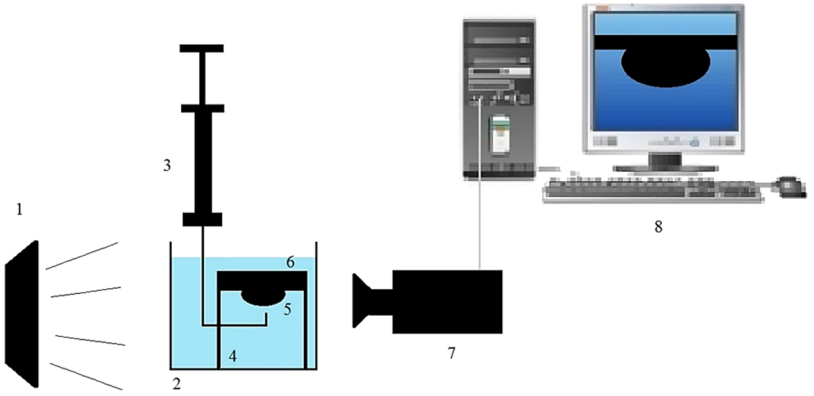

Figure 4. Schematic diagram illustrating the setup of the contact angle measurement device. (1) Light source, (2) cell, (3) syringe and needle, (4) holder, (5) drop, (6) thin section, (7) camera, and (8) computer.

nanofluids were stirred on a magnetic stirrer for 30 min and then underwent ultrasonic radiation for 30 min using a 200 W Hielscher UP200H ultrasonic device to obtain homogeneous and stable nanofluid solutions. In addition, the electrical conductivity of the prepared nanofluids at different concentrations was measured to evaluate the ionic strength of nanofluids. To measure the electrical conductivity of solutions, a cond7310 conductivity meter was used.

2.5. Surface Tension and Interfacial Tension Measurements. Interfacial tension tests between two liquids and surface tension between a liquid and a gas at different concentrations of solutions were measured at ambient temperature and pressure using the pendant drop technique. As shown in Figure 3, the IFT was measured by a device including a glass cell, a jack for height adjustment, a hand syringe pump for droplet injection, a light source, a camera, and a movable stand for adjusting the camera distance from the glass cell. The images of this device were analyzed by image processing software, and the IFT values were obtained. The VIT 6000 Fars EOR Technologies device was used to measure ST in this study. This device has an inlet for bulk fluid (CO_2 gas) and an inlet for droplet injection. The insulation chamber of this device makes it possible to measure ST under different temperatures and pressures. The images of this device were also transferred to the computer by a camera and analyzed with image processing software. Figure 3 shows the schematic illustration of the setup of IFT and ST measurements.

To measure the IFT, the device's glass cell was first filled with bulk fluid (nanofluid). The oil drop was then hung from the tip of a needle in the bulk fluid, and the camera captured a moment-by-moment photo and sent it to the software for calculation. For the ST test, the insulation chamber of the VIT 6000 was filled with a bulk fluid (CO_2 gas) and then a drop of nanofluid was hung from the tip of a needle into the chamber filled with CO_2 gas, and the images were sent to the computer by the camera. The pendant drop technique used for the measurements in this study depends on the following hypotheses.

- The droplet of crude oil should be symmetrical and suspended within the center of the vertical axis.
- The crude oil droplet should be static under the impact of gravity and interfacial tension forces.[44]

In this method, IFT and ST are easily calculated from the estimated dimensions of a droplet. The large droplet diameter (D) and the small droplet diameter (d) from the top of the droplet to the base at distance D are necessary parameters that were measured (see Figure 3). The software also processes images of these two devices using the following equation to calculate the IFT and ST (σ).[44]

$$\sigma = \frac{\Delta\rho g D}{H} \tag{1}$$

where $\Delta\rho$ is the difference between the two fluid densities, g is the gravitational acceleration, and H is the drop shape coefficient that is calculated from large and small diameters of the droplet by software.[34]

2.6. Contact Angle Measurement. A primary source of data for wettability studies is contact angle measurement. The contact angle, which is the angle between the contact surface of a rock and a fluid, actually indicates the wetting degrees of solid–liquid interactions.[33] The sessile drop technique was used to measure the contact angle of the oil droplet on the surface of

https://doi.org/10.1021/acsomega.2c03076
ACS Omega 2022, 7, 36165−36174

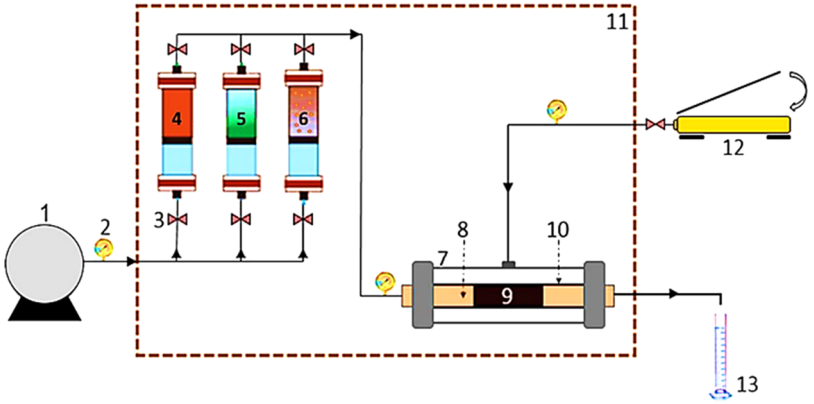

Figure 5. Schematic illustration of the coreflooding apparatus. (1) HPLC pump, (2) barometer, (3) valve, (4) cylinder containing crude oil, (5) saline-water-containing cylinder, (6) cylinder containing nanofluid, (7) core holder chamber, (8) fluid flow distributor, (9) core, (10) blocking rubber around the core, (11) oven, (12) manual hydraulic pump, and (13) outlet fluid collecting vessel.[13] Reprinted with permission from [Ali, et al., 2019].[13] Copyright [2019/Energy & Fuels] [American Chemical Society].

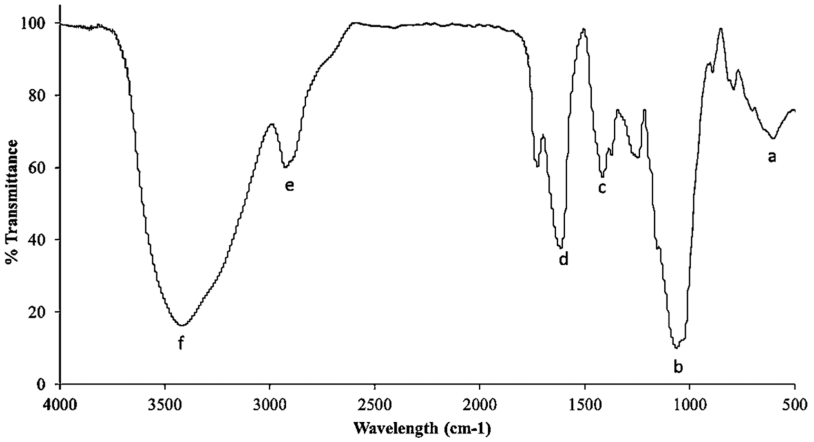

Figure 6. FTIR spectrum pattern of the nanocomposites. Reprinted with permission from [Ali, et al., 2022].[47] Copyright [2022/Energy & Fuels] [American Chemical Society].

rock pellets in the presence of nanofluids based on the drop shape development theory (see Figure 4). For this purpose, the core plugs were cut into different pellets, and the prepared pellets were smoothened and polished well. Afterward, they were washed well with distilled water and toluene. The cleaned-dried pellets were submerged and kept within the crude oil for four weeks to develop the oil-wet state.

After the thin sections in the crude oil aged and became completely oil-wet, we placed these thin sections in nanofluid solutions for one day to alter their wettability. After one day, we removed the sections from the solutions, and to measure the contact angle of each of them, we placed the desired thin sections on the holder of the contact angle device and filled the glass container of the device with the desired solution. After filling the glass chamber with the desired solution and placing the thin section in the chamber, a drop of crude oil was released from under the thin section to its surface by a hand syringe pump. At this point, the camera took a photo of the thin section and sent it to the computer for processing by software and measuring of the contact angle.

2.7. Oil Displacement. To evaluate the EOR potential of KCl/SiO_2/Xanthan NCs, a coreflooding test was performed. To inject the fluids into the prepared core plugs, a coreflooding setup shown in Figure 5 was used. This device can perform the oil displacement test through the core plug with length 3.5″ and diameter 1.5″ under different pressure and temperature conditions. Fluids can be pumped by automatic pumps that are installed directly behind the cylinders that contain particular aqueous phases to the core chambers and then core plugs with the adjustable rate. The core holder is covered by a rubber that can be pressed hydraulically around the plugs to arrest unwanted flow around the core plugs.[44] The core plug, prepared from the collected carbonate rock samples, was washed using the Soxhlet apparatus and aged to represent the reservoir condition using the coreflooding device under pressure and temperature for 2 weeks. In this step, OOIP and S_{W_i} can be calculated using eqs 2 and 3. Afterward, secondary recovery was performed by injecting seawater into the core and measuring the oil produced from the outlet. The injection of seawater was continued until oil production stopped and reached 99% of the water cut, at which time the secondary oil recovery process was considered to have been complete. When no more oil was produced from the core in the seawater injection, tertiary oil recovery was performed. The process of tertiary oil recovery was exactly the same as the secondary oil recovery process, except that at this stage, nanofluid at an optimum concentration of the synthesized NCs was injected into the core instead of seawater. During this process, pressure, injection time, injection volume, and the amount of oil produced were measured to calculate the recovery factor. All stages of the coreflooding test were performed at an

https://doi.org/10.1021/acsomega.2c03076
ACS Omega 2022, 7, 36165−36174

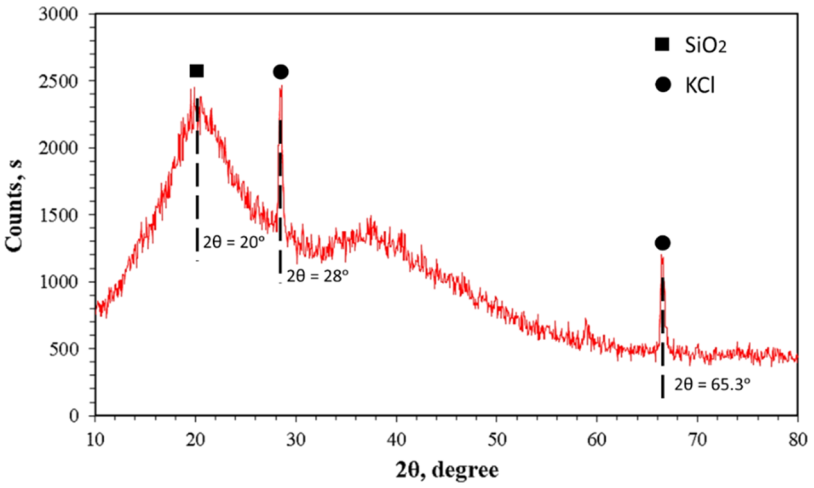

Figure 7. XRD pattern of green synthesized SiO_2/KCL/Xanthan NCs. Reprinted with permission from [Ali, et al., 2022].[47] Copyright [2022/Energy & Fuels] [American Chemical Society].

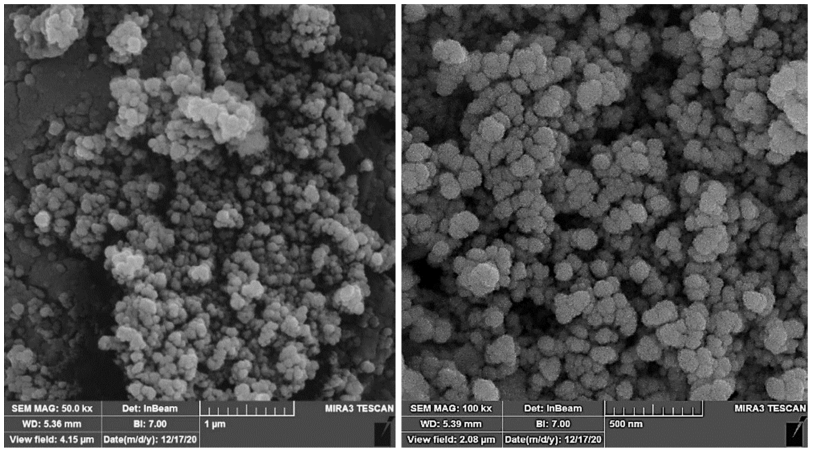

Figure 8. SEM of the synthesized NCs at 50 kx (1 um) and 100 kx (500 um) magnifications. Reprinted with permission from [Ali, et al., 2022].[47] Copyright [2022/Energy & Fuels] [American Chemical Society].

injection rate of 0.5 cm^3/min at 1400 psi pressure and 75 °C temperature.

$$\text{OOIP} = \text{brine production} \tag{2}$$

$$S_{W_i} = \text{pore volume} - \text{brine production} \tag{3}$$

3. RESULTS AND DISCUSSION

3.1. Characterization of Nanocomposites. The FTIR spectrum of the synthesized nanocomposites is shown in Figure 6. As can be seen, Figure 6 demonstrates the presence of the phytochemical compounds of the NCs that contain several main peaks [a−e]. Signals a−c with wavelengths of 600, 1050, and 1450 cm^{-1} represent the bending of C−C, stretching of C−O, and double stretching of C═C, respectively. However, the double stretching bond of C═O, the third stretching bond of C−H, and the single stretching of O−H were identified at wavelengths of 1600, 2800, and 3420 cm^{-1}, respectively. Thus, the presence of the organic functional groups within synthesized SiO_2/KCl/Xanthan NCs can be confirmed. In addition, the XRD pattern that contains three main peaks at $2\theta = 20°$, $2\theta = 28°$, and $\theta = 65.3°$ to prove the presence of SiO_2 and KCl in the synthesized NCs is illustrated in Figure 7. As is obvious, all related peaks of SiO_2 in terms of crystallinity and limpness of the used KCl and xanthan gum are detected on the XRD pattern. However, the amorphous phase of SiO_2 was defined by a broad peak on the XRD pattern obtained for the synthesized NCs, which evidences the presence of tiny particles along with their inner structure. SEM micrographs of green NCs are also determined, as shown in Figure 8. As can be seen, particles with a spherical shape were identified on both SEM images taken at different magnifications. According to Hernández et al.,[47] the detected spherical shape evidences the availability of SiO_2, which can prove advantageous for its use in porous media. In addition, silica nanoparticles along with KCl were clearly distributed on the polymer chains of xanthan as a substrate to fabricate the nanocomposites. NPs with sizes ranging within the scale of manometers were observed on the SEN depending on the scale bar of the micrographs.

3.2. Electrical Conductivity. The electrical conductivity of the prepared nanofluids was measured at different concentrations. As shown in Figure 9, on increasing the concentration of NCs, the electrical conductivity of nanofluids shows an upward trend. Although this is an upward trend, its slope decreases at high concentrations. The optimal concentration of the NCs can be determined from the point of contact of the trend lines drawn in the graph of electrical conductivity against the NC concentration. In this sample, the optimum concen-

https://doi.org/10.1021/acsomega.2c03076
ACS Omega 2022, 7, 36165−36174

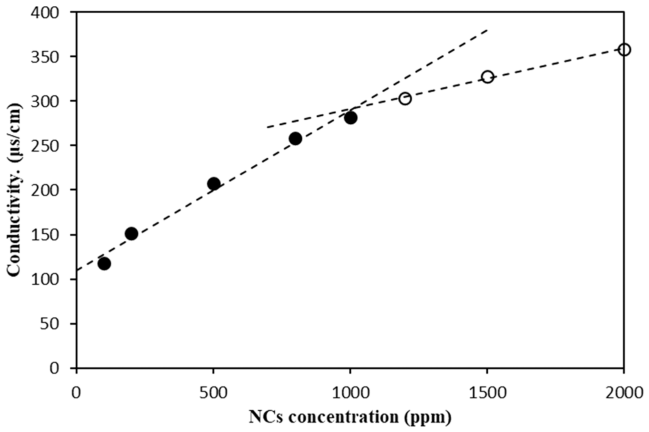

Figure 9. Electrical conductivity measured for the formulated nanofluids.

tration of the synthesized NCs is 1000 ppm. This means that increasing the concentration of nanocomposites to more than 1000 ppm, increasing the agglomeration rate of nanocomposite particles, and their early deposition in the nanofluid can prevent the increase of electrical conductivity with a constant slope. Therefore, nanocomposite concentrations greater than 1000 ppm are not expected to be suitable for use in EOR.

3.3. Surface and Interfacial Tensions. IFT reduction is a powerful mechanism in EOR that has a direct impact on oil flow in a porous medium and the release of trapped oils. Decreased IFT leads to decreased capillary forces, increased capillary number, and ultimately increased oil recovery.[38] According to the investigations of Li et al.[50] and Dahle et al.,[51] nanoparticles form a layer-like structure on the surface between nanofluids and crude oil. This layer acts quite similar to surfactants as a mediator and reduces IFT.[49−53] As the concentration of nanoparticles increases, this mechanism becomes stronger and further reduces the IFT. Although individual nanoparticles can reduce the IFT, many recent studies have shown that nanocomposites have a greater ability to reduce IFT. This ability of nanocomposites is due to the synergistic effect of nanocomposite components in reducing IFT with common polymers covering them. IFT reduction is clearly not the main and primary mechanism of nanoparticles and nanocomposites in EOR, unlike other CEOR methods, especially in reservoirs at harsh conditions such as high-pressure reservoirs.

Dynamic IFT and ST of nanofluids were measured by the pendant drop method at ambient temperature and pressure. After the IFT/ST of each solution reached a constant value in the IFT/ST change graph vs time, this constant value was considered the solution IFT/ST at that concentration. The results of equilibrium IFT and ST of nanofluids at different concentrations are given in Table 4. Figure 10 shows the IFT diagram of nanofluids at different concentrations. As shown in the diagram, the addition of nanocomposites to distilled water reduces its IFT. This decrease in IFT occurres up to a nanocomposite concentration of 1000 ppm, but a further increase in the concentration of nanocomposites shows the

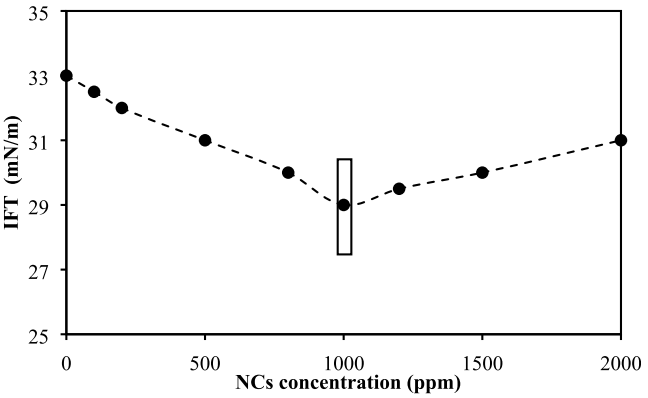

Figure 10. IFTs values measured for the crude/nanofluid systems at different concentrations.

opposite behavior and increases the IFT. Therefore, the nanocomposite concentration of 1000 ppm can be considered the optimal concentration for reducing IFT. In general, the performance of this nanocomposite in reducing IFT is poor, and at maximum, it has been able to reduce the IFT from 33 to 29 mN/m and reduce it by only 12%. It can be said that the performance of nanoparticles in ST is the same as that in IFT and follows the same mechanisms. The results of nanofluid ST at different concentrations are also shown in Figure 11. In this case,

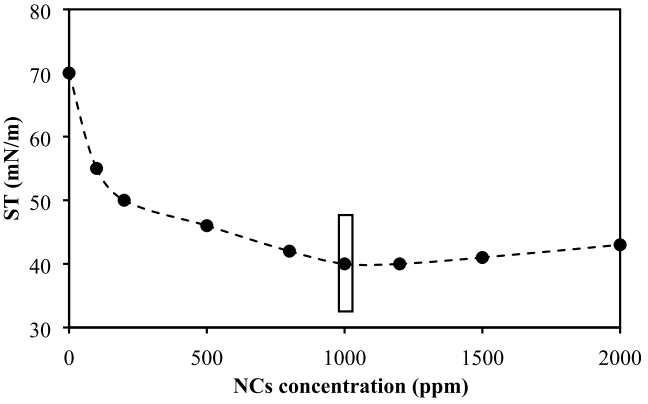

Figure 11. IFT values measured for the gas/nanofluid systems at different concentrations.

too, increasing the nanocomposite concentration to 1000 ppm reduces the ST value from 70 to 40 mN/m, and as the nanocomposite concentration increases further, the ST value increases slightly. It can be concluded that the synthesized nanocomposites show better performance in dealing with CO_2 gas than dealing with crude oil and are able to reduce ST by 43%.

3.4. Contact Angle. Nanoparticles alter wettability by being absorbed on the rock and forming a thin film on its surface. This thin film spreads on the surface of the rock with a wettability effect opposite to the initial wettability of the rock and removes the adhered oil and hydrocarbon compounds from its surface, which leads to an alteration in the wettability of the rock surface.

Table 4. IFT and ST of the Formulated Nanofluids

NCs concentration (ppm)	0	100	200	500	800	1000	1200	1500	2000
IFT (mN/m)	33	32.5	32	31	30	29	29.5	30	31
ST (mN/m)	70	55	50	46	42	40	40	41	43

https://doi.org/10.1021/acsomega.2c03076
ACS Omega 2022, 7, 36165−36174

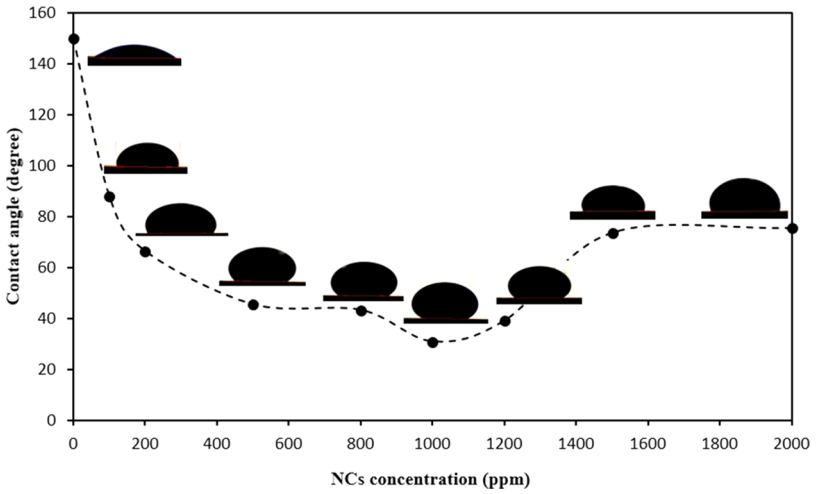

Figure 12. Contact angle of the oil droplet on the surface of the carbonate rock in the presence of the nanofluid at different concentrations.

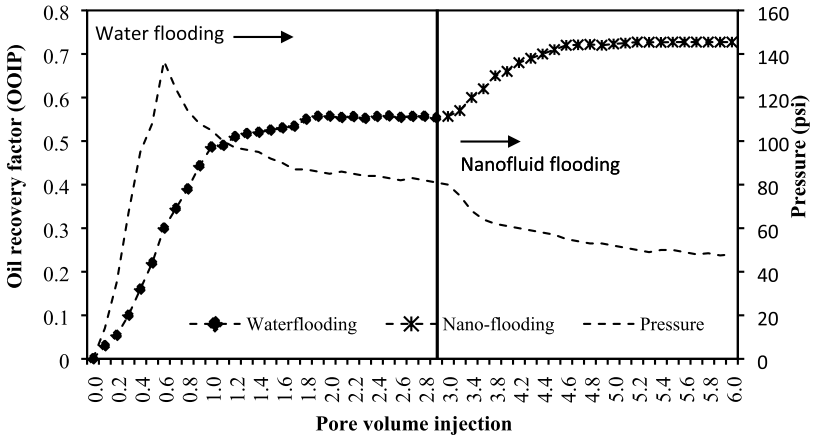

Figure 13. Pressure and oil recovery factor profiles of the coreflooding test; waterflooding (secondary injection) and nanofluid injection (tertiary recovery).

The intensity of this phenomenon depends on the properties of nanofluids and nanoparticles in it compared with those of the fluid and reservoir rock.[38] The adsorption of nanoparticles on the rock surface can be due to the electrostatic forces between the nanoparticles and the rock surface. Figure 12 shows the contact angle diagram of nanofluids at different nanocomposite concentrations along with the image of oil droplets on the rock surface. As shown in the figure, increasing the nanocomposite concentration to 1000 ppm could reduce the contact angle, but further increase in the concentration of nanocomposites increases the contact angle again. By increasing the nanocomposite concentration to 1000 ppm, in fact, the adsorption of nanoparticles on the positively charged surface of the carbonate rock increases and a stronger film is formed on its surface, which reduces the contact angle. Further increase in nanocomposite concentration after 1000 ppm leads to an increase in irregular movements of nanoparticles and an increase in system entropy and finally an increase in contact angle. Therefore, a concentration of 1000 ppm was considered as the optimal concentration of this nanocomposite and was used for injection in the EOR process. At its optimum concentration, the synthesized NC could reduce the contact angle from 150.1 to 30.8° and optimize the wettability by 79.5%.

3.5. Oil Displacement. The coreflooding test was performed on a carbonate core plug with the characteristics given in Table 3. The initial water saturation after the aging was 32.74%, with an OOIP of 4.4 cc. When the water was injected, an increase in the oil recovery and pressure was obtained, as shown in Figure 13. At the end of the seawater injection phase, a secondary recovery of 55.68% was obtained at 3 PVs. Then, the nanofluid was injected into the core with a nanocomposite concentration of 1000 ppm as the tertiary injection. At the end of the tertiary phase, the final recovery reached 72.73%, which shows that the injection of the nanofluid was able to increase the recovery by 17.05%. Seawater injection produced oil from the core with a slight alteration in wettability due to the presence of ions and an increase in system pressure as a sweeping effect, but nanofluid injection through both IFT reduction and optimization of wettability alteration mechanisms resulted in residual oil production and increased oil recovery.

3.6. Economic Feasibility of Using SiO_2/KCl/Xanthan Nanocomposites. The main aim of implementing EOR projects is to increase the cumulative production rate from oil reservoirs and the total revenue of the oilfield. For a successful project, all of the necessary steps of the design, the cost, the implementation procedure, and material fabrication should be carefully managed. The main CEOR mechanisms are IFT reduction and wettability alteration. A green nanocomposite of SiO_2/KCl/Xanthan was synthesized from the extract of the *E. condylocarpa* plant. Adding the fabricated NCs to water leads to a

https://doi.org/10.1021/acsomega.2c03076
ACS Omega 2022, 7, 36165−36174

great reduction in the value of IFT, alteration of the wettability strongly from oil-wet to water-wet, and enables extraction of an extra 17% OOIP. Nanomaterials with very low concentrations have a significant influence on the EOR mechanisms and oil recovery. It can be recommended that nanoparticles and nanomaterials be applied in real oilfields for achieving enhanced oil recovery.

4. CONCLUSIONS

In this study, the effect of the new synthetic nanocomposites called KCl/SiO_2/Xanthan on the EOR process was investigated. Several EOR experimental tests were carried out on nanofluid solutions to determine the performance of KCl/SiO_2/Xanthan NCs. The most important conclusions of this study are summarized as follows.

- XRD, FTIR, and SEM results confirmed the validity of KCl/SiO_2/Xanthan NCs.
- The nanofluid with 1000 ppm KCl/SiO_2/Xanthan NCs was ineffective in reducing the IFT; however, it was effective in decreasing the ST from 70 to 40 mN/m.
- The nanofluid made from 1000 ppm KCl/SiO_2/Xanthan NCs could alter the wettability of the rock from strong oil-wet to water-wet.
- Therefore, the synthesized NC was effective in increasing the oil recovery by an extra 17.05% OOIP and showed acceptable performance in EOR.

AUTHOR INFORMATION

Corresponding Authors

Abbas Khaksar Manshad − *Department of Petroleum Engineering, Abadan Faculty of Petroleum, Petroleum University of Technology (PUT), Abadan 6318714331, Iran; Department of Petroleum Engineering, Faculty of Engineering, Soran University, Soran 44008 Kurdistan Region, Iraq*; Email: khaksar@put.ac.ir

Amir H. Mohammadi − *Discipline of Chemical Engineering, School of Engineering, University of KwaZulu-Natal, Durban 4041, South Africa*; orcid.org/0000-0002-2947-1135; Email: amir_h_mohammadi@yahoo.com

Authors

Ali Ahmadi − *Department of Petroleum Engineering, Abadan Faculty of Petroleum, Petroleum University of Technology (PUT), Abadan 6318714331, Iran*

Jagar A. Ali − *Department of Petroleum Engineering, Faculty of Engineering, Soran University, Soran 44008 Kurdistan Region, Iraq; Department of Geology, Palacký University, Olomouc 77146, Czech Republic*; orcid.org/0000-0002-7327-4243

Stefan Iglauer − *Discipline of Petroleum Engineering, School of Engineering, Edith Cowan University, Joondalup 6027 Western Australia, Australia*; orcid.org/0000-0002-8080-1590

S. Mohammad Sajadi − *Department of Nutrition, Cihan University—Erbil, Erbil, Kurdistan 44001, Iraq*

Alireza Keshavarz − *Discipline of Petroleum Engineering, School of Engineering, Edith Cowan University, Joondalup 6027 Western Australia, Australia*; orcid.org/0000-0002-8091-961X

Complete contact information is available at: https://pubs.acs.org/10.1021/acsomega.2c03076

Notes

The authors declare no competing financial interest.

ACKNOWLEDGMENTS

This project was supported by the Soran University and the Petroleum University of Technology in terms of material and facility provision.

REFERENCES

(1) Haq, B. Green enhanced oil recovery for carbonate reservoirs. *Polymers* **2021**, *13*, No. 3269.

(2) Davoodi, S.; Al-Shargabi, M.; Wood, D. A.; Rukavishnikov, V. S.; Minaev, K. M. Experimental and field applications of nanotechnology for enhanced oil recovery purposes: A review. *Fuel* **2022**, *324*, No. 124669.

(3) Cheraghian, G.; Tardasti, S. In *Improved Oil Recovery by the Efficiency of Nano-particle in Imbibition Mechanism*, Conference Proceedings, 2nd EAGE International Conference KazGeo; European Association of Geoscientists & Engineers, 2012.

(4) Emadi, S.; Shadizadeh, S. R.; Manshad, A. K.; Rahimi, A. M.; Nowrouzi, I.; Mohammadi, A. H. Effect of Using Zyziphus Spina Christi or Cedr Extract (CE) as a Natural Surfactant on Oil Mobility Control by Foam Flooding. *J. Mol. Liq.* **2019**, *293*, No. 111573.

(5) Almajid, M. M.; Kovscek, A. R. Pore-Level Mechanics of Foam Generation and Coalescence in the Presence of Oil. *Adv. Colloid Interface Sci.* **2016**, *233*, 65−82.

(6) Alyousef, Z.; Almobarky, M.; Schechter, D. Enhancing the Stability of Foam by the Use of Nanoparticles. *Energy Fuels* **2017**, *31*, 10620−10627.

(7) Kumar, S.; Mandal, A. Investigation on Stabilization of CO_2 Foam by Ionic and Nonionic Surfactants in Presence of Different Additives for Application in Enhanced Oil Recovery. *Appl. Surf. Sci.* **2017**, *420*, 9−20.

(8) Manan, M. A.; Farad, S.; Piroozian, A.; Esmail, M. J. A. Effects of Nanoparticle Types on Carbon Dioxide Foam Flooding in Enhanced Oil Recovery. *Pet. Sci. Technol.* **2015**, *33*, 1286−1294.

(9) Alsaba, M. T.; Dushaishi, M. F. A.; Abbas, A. K. A Comprehensive Review of Nanoparticles Applications in the Oil and Gas Industry. *J. Pet. Explor. Prod. Technol.* **2020**, *10*, 1389−1399.

(10) Yekeen, N.; Manan, M. A.; Idris, A. K.; Padmanabhan, E.; Junin, R.; Samin, A. M.; Gbadamosi, A. O.; Oguamah, I. A Comprehensive Review of Experimental Studies of Nanoparticles-Stabilized Foam for Enhanced Oil Recovery. *J. Pet. Sci. Eng.* **2018**, *164*, 43−74.

(11) Ali, J. A.; Kolo, K.; Manshad, A. K.; Mohammadi, A. H. Recent Advances in Application of Nanotechnology in Chemical Enhanced Oil Recovery: Effects of Nanoparticles on Wettability Alteration, Interfacial Tension Reduction, and Flooding. *Egypt. J. Pet.* **2018**, *27*, 1371−1383.

(12) Ali, J. A.; Manshad, A. K.; Imani, I.; Sajadi, S. M.; Keshavarz, A. Greenly Synthesized Magnetite@SiO_2@Xanthan Nanocomposites and Its Application in Enhanced Oil Recovery: IFT Reduction and Wettability Alteration. *Arabian J. Sci. Eng.* **2020**, *45*, No. 7863.

(13) Ali, J. A.; Kolo, K.; Manshad, A. K.; Stephen, K. D. Low-salinity polymeric nanofluid-enhanced oil recovery using green polymer-coated ZnO/SiO_2/Nanocomposites in the upper Qamchuqa formation in Kurdistan region, Iraq. *Energy Fuels* **2019**, *33*, 927−937.

(14) Alizadeh, A. H.; Keshavarz, A.; Haghighi, M. In *Flow Rate Effect on Two-Phase Relative Permeability in Iranian Carbonate Rocks*, SPE Middle East Oil and Gas Show and Conference, 2007.

(15) Kazemzadeh, Y.; Parsaei, R.; Riazi, M. Experimental Study of Asphaltene Precipitation Prediction during Gas Injection to Oil Reservoirs by Interfacial Tension Measurement. *Colloids Surf., A* **2015**, *466*, 138−146.

(16) Fanchi, J. R.*Shared Earth Modeling*; Gulf Professional Publishing: Amsterdam, 2002.

(17) Zargartalebi, M.; Kharrat, R.; Barati, N. Enhancement of Surfactant Flooding Performance by the Use of Silica Nanoparticles. *Fuel* **2015**, *143*, 21−27.

(18) Bayda, S.; Adeel, M.; Tuccinardi, T.; Cordani, M.; Rizzolio, F. The History of Nanoscience and Nanotechnology: From Chemical−Physical Applications to Nanomedicine. *Molecules* **2020**, *25*, No. 112.
(19) Ragab, A. M.; Hannora, A. E. In *An Experimental Investigation of Silica Nano Particles for Enhanced Oil Recovery Applications*, SPE North Africa Technical Conference and Exhibition, 2015.
(20) Sun, Y.; Yang, D.; Shi, L.; Wu, H.; Cao, Y.; He, Y.; Xie, T. Properties of Nanofluids and Their Applications in Enhanced Oil Recovery: A Comprehensive Review. *Energy Fuels* **2020**, *34*, 1202−1218.
(21) Nowrouzi, I.; Manshad, A. K.; Mohammadi, A. H. Effects of TiO2, MgO, and γ-Al_2O_3 Nano-Particles in Carbonated Water on Water-Oil Interfacial Tension (IFT) Reduction in Chemical Enhanced Oil Recovery (CEOR) Process. *J. Mol. Liq.* **2019**, *292*, No. 111348.
(22) Cheraghian, G.; Rostami, S.; Afrand, M. Nanotechnology in Enhanced Oil Recovery. *Processes* **2020**, *8*, No. 1073.
(23) Yekeen, N.; Manan, M. A.; Idris, A. K.; Samin, A. M.; Risal, A. R. Experimental Investigation of Minimization in Surfactant Adsorption and Improvement in Surfactant-Foam Stability in Presence of Silicon Dioxide and Aluminum Oxide Nanoparticles. *J. Pet. Sci. Eng.* **2017**, *159*, 115−134.
(24) Yu, J.; An, C.; Mo, D.; Liu, N.; Lee, R. In *Study of Adsorption and Transportation Behavior of Nanoparticles in Three Different Porous Media*, SPE Improved Oil Recovery Symposium, 2012.
(25) Huang, F.; Kang, Y.; You, Z.; You, L.; Xu, C. Critical Conditions for Massive Fines Detachment Induced by Single-Phase Flow in Coalbed Methane Reservoirs: Modeling and Experiments. *Energy Fuels* **2017**, *31*, 6782−6793.
(26) Ali, J. A.; Kalhury, A. M.; Sabir, A. N.; Ahmed, R. N.; Ali, N. H.; Abdullah, A. D. A state-of-the-art review of the application of nanotechnology in the oil and gas industry with a focus on drilling engineering. *J. Pet. Sci. Eng.* **2020**, *191*, No. 107118.
(27) Kazemzadeh, Y.; Shojaei, S.; Riazi, M.; Sharifi, M. Review on Application of Nanoparticles for EOR Purposes: A Critical Review of the Opportunities and Challenges. *Chin. J. Chem. Eng.* **2019**, *27*, 237−246.
(28) Ragab, A. M. S.; Hannora, A. E. In *A Comparative Investigation of Nano Particle Effects for Improved Oil Recovery − Experimental Work*, SPE Kuwait Oil and Gas Show and Conference, **2015**.
(29) Cheraghian, G.; Rostami, S.; Afrand, M. Nanotechnology in enhanced oil recovery. *Processes* **2020**, *8*, No. 1073.
(30) Davarpanah, A. Parametric study of polymer-nanoparticles-Assisted Injectivity performance for axisymmetric two-phase flow in EOR processes. *Nanomaterials* **2020**, *10*, No. 1818.
(31) Dehdari, B.; Parsaei, R.; Riazi, M.; Rezaei, N.; Zendehboudi, S. New insight into foam stability enhancement mechanism, using polyvinyl alcohol (PVA) and nanoparticles. *J. Mol. Liq.* **2020**, *307*, No. 112755.
(32) Khalilinezhad, S. S.; Cheraghian, G.; Roayaei, E.; Tabatabaee, H.; Karambeigi, M. S. Improving heavy oil recovery in the polymer flooding process by utilizing hydrophilic silica nanoparticles. *Energy Sources, Part A* **2017**, *1*, 1−10.
(33) Negin, C.; Ali, S.; Xie, Q. Application of Nanotechnology for Enhancing Oil Recovery − A Review. *Petroleum* **2016**, *2*, 324−333.
(34) Bila, A.; Torsæter, O. Experimental Investigation of Polymer-Coated Silica Nanoparticles for EOR under Harsh Reservoir Conditions of High Temperature and Salinity. *Nanomaterials* **2021**, *11*, No. 765.
(35) Ju, B.; Fan, T. Experimental Study and Mathematical Model of Nanoparticle Transport in Porous Media. *Powder Technol.* **2009**, *192*, 195−202.
(36) Qi, L.; Song, C.; Wang, T.; Li, Q.; Hirasaki, G. J.; Verduzco, R. Polymer-Coated Nanoparticles for Reversible Emulsification and Recovery of Heavy Oil. *Langmuir* **2018**, *34*, 6522−6528.
(37) Behzadi, A.; Mohammadi, A. Environmentally Responsive Surface-Modified Silica Nanoparticles for Enhanced Oil Recovery. *J. Nanopart. Res.* **2016**, *18*, No. 266.
(38) Taleb, M.; Sagala, F.; Hethnawi, A.; Nassar, N. N. Enhanced oil recovery from Austin chalk carbonate reservoirs using faujasite-based nanoparticles combined with low-salinity water flooding. *Energy Fuels* **2021**, *35*, 213−225.
(39) Rayeni, N. S.; Imanivarnosfaderani, M.; Rezaei, A.; Gomari, S. R. An experimental study of the combination of smart water and silica nanoparticles to improve the recovery of asphaltenic oil from carbonate reservoirs. *J. Pet. Sci. Eng.* **2022**, *208*, No. 109445.
(40) Shahrabadi, A.; Daghbandan, A.; Arabiyoun, M. Experimental investigation of the adsorption process of the surfactant-nanoparticle combination onto the carbonate reservoir rock surface in the enhanced oil recovery (EOR) process. *Chem. Thermodyn. Therm. Anal.* **2022**, *6*, No. 100036.
(41) Jalilian, M.; Tabzar, A.; Ghasemi, V.; Mohammadzadeh, O.; Pourafshary, P.; Rezaei, N.; Zendehboudi, S. An experimental investigation of nanoemulsion enhanced oil recovery: Use of unconsolidated porous systems. *Fuel* **2019**, *251*, 754−762.
(42) Jafarbeigi, E.; Salimi, F.; Kamari, E.; Mansouri, M.Effects of modified graphene oxide (GO) nanofluid on wettability and IFT changes: Experimental study for EOR applications*Pet. Sci.*2021 DOI: 10.1016/j.petsci.2021.12.022.
(43) Soliman, A. A.; El-hoshoudy, A. N.; Attia, A. M. Assessment of xanthan gum and xanthan-G-silica derivatives as chemical flooding agents and rock wettability modifiers. *Oil Gas Sci. Technol. - Rev. Energ. nouv.* **2020**, *75*, No. 12.
(44) Zargar, G.; Arabpour, T.; Manshad, A. K.; Ali, J. A.; Sajadi, S. M.; Keshavarz, A.; Mohammadi, A. H. Experimental investigation of the effect of green TiO_2/Quartz nanocomposite on interfacial tension reduction, wettability alteration, and oil recovery improvement. *Fuel* **2020**, *263*, No. 116599.
(45) Ali, J. A.; Kolo, K.; Manshad, A. K.; Stephen, K. D. Emerging applications of TiO_2/SiO_2/poly(acrylamide) nanocomposites within the engineered water EOR in carbonate reservoirs. *J. Mol. Liq.* **2021**, *322*, No. 114943.
(46) Dashtaki, S. R. M.; Ali, J. A.; Manshad, A. K.; Nowrouzi, I.; Mohammadi, A. H.; Keshavarz, A. Experimental investigation of the effect of Vitagnus plant extract on enhanced oil recovery process using interfacial tension (IFT) reduction and wettability alteration mechanisms. *J. Pet. Explor. Prod. Technol.* **2020**, *10*, 2895−2905.
(47) Ali, J. A.; Hamadamin, A. B.; Ahmed, S. M.; Mahmood, B. S.; Sajadi, S. M.; Manshad, A. K. Synergistic effect of Nanoinhibitive drilling fluid on the shale swelling performance at high temperature and high pressure. *Energy Fuels* **2022**, *36*, 1996−2006.
(48) Hernández, A.; Barrios, M.; Sánchez, M. Synthesis and characterization of SiO_2 particles for the development of a novel sun skin protector enriched with antioxidants. *Mater. Today: Proc.* **2019**, *13*, 446−451.
(49) Bahraminejad, H.; Manshad, A. K.; Riazi, M.; Ali, J. A.; Sajadi, S. M.; Keshavarz, A. CuO/TiO_2/PAM as a Novel Introduced Hybrid Agent for Water—Oil Interfacial Tension and Wettability Optimization in Chemical Enhanced Oil Recovery. *Energy Fuels* **2019**, *33*, 10547−10560.
(50) Li, S.; Hendraningrat, L.; Torsaeter, O. In *Improved Oil Recovery by Hydrophilic Silica Nanoparticles Suspension: 2-Phase Flow Experimental Studies*, International Petroleum Technology Conference, 2013.
(51) Hendraningrat, L.; Engeset, B.; Suwarno, S.; Torsæter, O. In *Improved Oil Recovery by Nanofluids Flooding: An Experimental Study*, SPE Kuwait International Petroleum Conference and Exhibition, 2012.
(52) Manshad, A. K.; Ali, J. A.; Haghighi, O. M.; Sajadi, S. M.; Keshavarz, A. Oil recovery aspects of ZnO/SiO_2 nano-clay in carbonate reservoir. *Fuel* **2022**, *307*, No. 121927.
(53) Dahle, G. S.The Effect of Nanoparticles on Oil/Water Interfacial Tension. Project thesis, NTNU, 2013.

https://doi.org/10.1021/acsomega.2c03076
ACS Omega 2022, 7, 36165−36174